International Research Journal of Innovations in Engineering and Technology (IRJIET)

ISSN (online): 2581-3048

Volume 10, Issue 9, pp 150-163, September-2026

https://doi.org/10.47001/IRJIET/2026.109016

Excitation Design and Guaranteed Robustness Bounds for Residuation-Based Identification of Max-Plus Linear Discrete Event Systems

Ghadir Aryan

Faculty of Information Engineering, University of Idlib, Idlib, Syria
École Centrale de Nantes, Nantes Cedex 3, France
E-mail: ghadir_hamdi_aryan@idlib.edu.sy

***Abstract* - Timed event graphs describe manufacturing lines, transport networks and computing pipelines governed by synchronisation and delay, and they are linear over the max-plus dioid. Estimating their temporal parameters from one record of input and output firing dates is classically solved by residuation, which returns the greatest parameter vector whose predicted output never exceeds the measured one. This paper establishes when that estimator is trustworthy. First, a parameter is recovered exactly if and only if its regressor attains the maximum in the measured output at least once; for constant-rate excitation this yields closed-form critical rates governed by the chord slopes of the transient block, not by the eigenvalue as previously assumed, the eigenvalue governing only the periodic block. Second, the minimum record length is obtained in closed form and diverges as the excitation rate approaches the eigenvalue, which shows that the reported insensitivity to record length is an artefact of testing far from the critical rate. Third, the estimator is proved non-expansive with respect to timestamp errors, and under non-negatively biased timestamps the identified model is proved to be a guaranteed upper bound on the true system, so predicted completion dates are never optimistic. A campaign on two plants comprising more than seven thousand runs confirms every statement: the exactness criterion reproduces recovery in sixty of sixty cases, the record-length law holds in eighteen of nineteen configurations, and conservativeness is observed in all two thousand four hundred one-sided runs against none under symmetric errors. Excitation design rules follow.**

Keywords: max-plus algebra, dioid, timed event graph, discrete event system, system identification, residuation, identifiability, experiment design, robustness, manufacturing systems.

NOMENCLATURE

Symbol	**Meaning**
DES	discrete event system
TEG	timed event graph
SISO	single input, single output
$\oplus$, $\otimes$	max-plus addition (maximum) and multiplication (sum)
ε, e	zero and unit of the dioid, $-\infty$ and 0
$\preceq$	order induced by idempotent addition
γ	backward shift operator on the event index
u(k), y(k)	dates of the k-th input and output firing
h	transfer series of the graph
p, q, s, r, v	transient block, periodic block, period duration, period in events, transient length
λ=s/r	eigenvalue, asymptotic interval between output firings
θ, $\hat{\theta}$	true and estimated parameter vector
Φ	regression matrix
$\Phi\backslash$ Y	residual of max-plus matrix multiplication
J	one-sided fit criterion
N	number of observations in the record
δ	constant release interval of the input
δ*	critical release interval of the transient block

International Research Journal of Innovations in Engineering and Technology (IRJIET)

ISSN (online): 2581-3048

Volume 10, Issue 9, pp 150-163, September-2026

https://doi.org/10.47001/IRJIET/2026.109016

d	timestamp error on the output record

I. INTRODUCTION

Discrete event systems evolve through the occurrence of events at instants that need not be regularly spaced. When such a system is driven by synchronisation and delay but contains no conflict, it is naturally modelled by a timed event graph (TEG), a Petri net in which every place has exactly one upstream and one downstream transition. The decisive property of this class is that its dynamics, which are nonlinear in conventional algebra, become linear in the max-plus dioid [1], [2]. The algebraic groundwork goes back to minimax algebra [3]. Two decades of work have exploited this linearity to transpose control-theoretic constructions to discrete event systems: model-reference control [4], model predictive control [5] and its stochastic extension [6], observer design and observer-based control [7], [8], control under state restriction [9], disturbance decoupling [10], and robust design under parametric uncertainty using interval analysis over idempotent semirings [11], [12].

Every one of these constructions presupposes a model. Obtaining that model from data is therefore the enabling step, and it is considerably less developed than the control theory built on top of it. Section II reviews what is available.

1.1 Contribution

The paper makes four contributions.

1. **An exact identifiability criterion**. A parameter is recovered exactly if and only if its regressor is active, that is, attains the maximum in the measured output at some observation index (Theorem 2). The criterion is checkable in linear time on simulated data and is therefore usable as an experiment-design test.
2. **Closed-form critical excitation rates**. For a constant-rate input, the transient coefficients have individual critical rates given by the minimal chord slope of the transient sequence (Corollary 1), whereas the periodic block is governed by the eigenvalue (Corollary 2). The two thresholds are numerically different, and the smaller one determines complete identifiability. This corrects the commonly assumed single eigenvalue threshold.
3. **A record-length law**. The minimum number of observations required for complete identification is obtained in closed form (Proposition 3) and grows as the reciprocal of the distance between the excitation rate and the eigenvalue. Far from the eigenvalue the requirement collapses to one observation per parameter, which explains the reported insensitivity to record length.
4. **Two-sided robustness guarantees**. The estimator is non-expansive in the supremum norm with respect to timestamp perturbations (Theorem 3), and for non-negatively biased timestamps the identified transfer series dominates the true one (Theorem 4). Combining the two yields a sandwich bound: the identified model lies between the true model and the true model inflated by the worst-case timestamp error. Consequently, completion dates predicted from the identified model are never optimistic, which is precisely the property required for admissible scheduling.

All statements are validated on two plants over more than seven thousand identification runs. The complete implementation and every figure, table and number are reproducible from the accompanying code.

1.2 Organisation

Section II reviews the two families of identification methods available in the dioid setting. Section III fixes notation and states the estimation problem. Section IV develops the estimator and establishes the theoretical results. Section V reports the numerical study and converts the theory into excitation design rules. Section VI concludes and Section VII gives the future scope.

II. LITERATURE SURVEY

Two families of identification methods exist within the dioid setting. The first decomposes the impulse response into a finite sum of first-order elements and estimates the gain of each element by residuation [13], [14]. The second assumes the structural indices of the transfer series to be known and estimates the temporal parameters of a canonical periodic form [15]. Both reduce to the same algebraic operation: compute the greatest parameter vector whose predicted output remains below the measured output, which is exactly the residual of max-plus matrix multiplication [16], [17]. A separate line of work identifies discrete event systems as automata for fault-detection purposes [18]; it addresses logical rather than temporal behaviour and is

ISSN (online): 2581-3048
Volume 10, Issue 9, pp 150-163, September-2026
https://doi.org/10.47001/IRJIET/2026.109016

complementary to the present setting. The formal analogy with prediction-error identification of conventional linear systems [19] is close, but the algebra is different and so are the identifiability conditions, as shown below.

That operation always returns an answer. The question that has not been settled is when the answer is the right one. The available convergence statement [15] requires the excitation to be "sufficiently rich", a condition expressed through a residuated inequality that is not directly checkable and gives no guidance for designing an experiment. Empirical studies have suggested that the eigenvalue of the plant is the relevant threshold and that the length of the record has little influence. The present paper shows that the first suggestion is only half correct and that the second is a consequence of never testing near the critical regime.

III. PROBLEM DEFINITION

3.1 Dioids and the max-plus algebra

A *dioid* is a semiring whose addition is idempotent. Throughout, the scalar dioid is

$$Z_{\max} = (Z \cup \{-\infty\},\ \oplus,\ \otimes),\quad a \oplus b = \max(a,b),\quad a \otimes b = a + b,$$

with zero element ε=-∞ and unit element e=0. Idempotency induces the order

$$a \preceq b \Leftrightarrow a \oplus b = b,$$

which on $\mathbb{Z}_{\max}$ coincides with the natural order. The Kleene star of $a \in \mathbb{Z}_{\max}$ is $a^* = \bigoplus_{m\geq 0} a^m$.

Let $D[[\gamma]]$ denote the dioid of formal power series in the backward shift operator γ with coefficients in $\mathbb{Z}_{\max}$. Multiplying a series by γ shifts the event index by one, so γ plays the role of the z-transform variable for event-indexed signals.

3.2 Residuation

Isotone maps over complete dioids are generally not invertible, but the inequality $f(x) \preceq b$ possesses a greatest solution whenever f is residuable [13], [14]. For left multiplication by a matrix Φ, the greatest solution of $\Phi \otimes \theta \preceq Y$ is denoted $\Phi \backslash Y$ and is computed componentwise by

$$(\Phi \backslash Y)_l = \bigwedge_k (Y(k) - \Phi_l(k)) = \min_{k:\,\Phi_l(k)\neq\varepsilon} (Y(k) - \Phi_l(k)).$$

Equation (1) is the only computational tool used in this paper. Two elementary properties are recorded for later use: the map $Y \mapsto \Phi \backslash Y$ is isotone, and it is non-expansive in the supremum norm because a pointwise minimum of translates is.

3.3 Timed event graphs and the canonical periodic form

Let $u(k)$ and $y(k)$ denote the dates of the k-th firing of the input and output transitions of a single-input single-output TEG. The transfer series $h \in D[[\gamma]]$ satisfies $y = h \otimes u$, that is,

$$y(k) = \bigoplus_{j\geq 0} h(j) \otimes u(k-j) = \max_{0\leq j\leq k} (h(j) + u(k-j)).$$

It is known [1], [20] that h is ultimately periodic and can be written in the canonical form

$$h = p(\gamma)\ \oplus\ q(\gamma)(s\gamma^r)^*,\quad p(\gamma) = \bigoplus_{i=0}^{v-1} p_i\gamma^i,\quad q(\gamma) = \bigoplus_{j=0}^{r-1} q_j\gamma^{v+j},$$

where p describes the transient behaviour, q the repeated pattern, r the number of events in one period and s its duration. The ratio $\lambda = s/r$ is the eigenvalue of the plant, that is, the asymptotic time between two consecutive output firings, and λ^{-1} is the maximal throughput.

Introducing the internal variable $z = q(\gamma)(s\gamma^r)^* u$, (3) is equivalent to the state recursion

$$z(k) = s \otimes z(k-r)\ \oplus\ \bigoplus_{j=0}^{r-1} q_j \otimes u(k-v-j),\quad y(k) = \bigoplus_{i=0}^{v-1} p_i \otimes u(k-i)\ \oplus\ z(k),$$

International Research Journal of Innovations in Engineering and Technology (IRJIET)

ISSN (online): 2581-3048

Volume 10, Issue 9, pp 150-163, September-2026

https://doi.org/10.47001/IRJIET/2026.109016

with $u(k)=z(k)=\varepsilon$ for $k<0$. The structural indices v and r are integers fixed by the token distribution of the graph; the temporal parameters to be estimated are collected in the vector (5),

$$\theta=[p_0,\ \dots,p_{v-1},q_0,\ \dots,q_{r-1}]^\top\in Z_{\max}^{v+r}\ \text{togetherwith}\ s.$$

Assumption A1: The transient sequence is convex, that is, $p_{i+1}-p_i$ is non-decreasing in i.

Assumption A1 is not restrictive. Whenever h is realised as a finite sum of first-order elements, which is the case for every TEG obtained by parallel composition of routes, the coefficients of h are a pointwise maximum of affine functions of the event index and are therefore convex. All plants used in Section V satisfy A1 by construction.

IV. METHODOLOGY AND APPROACH

4.1 Regression form

Fix a candidate period duration $\sigma\geq 0$ and define the *starred regressor*

$$w_\sigma(k)=\left[(\sigma\gamma^r)^*u\right](k)=\max_{m\geq 0,\ k-mr\geq 0}(m\sigma+u(k-mr)).$$

With $\Phi_i(k)=u(k-i)$ for $0\leq i\leq v-1$ and $\Phi_{v+j}(k)=w_\sigma(k-v-j)$ for $0\leq j\leq r-1$, equation (4) becomes the linear regression

$$y(k)=\bigoplus_{l=0}^{v+r-1}\theta_l\otimes\Phi_l(k),\quad \text{i.e.}\quad Y=\Phi\otimes\theta$$

whenever $\sigma=s$. Given a record of length N, the estimate is the greatest parameter vector that does not overshoot the data,

$$\hat{\theta}(\sigma)=\Phi(\sigma)\backslash Y,\quad J(\sigma)=\sum_{k=0}^{N-1}\left(y(k)-\left[\Phi(\sigma)\otimes\hat{\theta}(\sigma)\right](k)\right)\ \geq\ 0,$$

and the period duration is selected as the greatest minimiser,

$$\hat{s}=\max\{\sigma\in S:J(\sigma)=\min J\},\quad S=\{0,\rho,2\rho,\ \dots,\sigma_{\max}\},$$

with grid step ρ and search bound $\sigma_{\max}=\max_{k\geq r}(y(k)-y(k-r))$. The bound is legitimate: if the periodic block is active at two indices separated by r, subtracting the corresponding identities gives $\sigma\leq y(k)-y(k-r)$.

Algorithm 1 (residuated structural identification). *Input:* records u,y of length N; structural indices v,r; grid step ρ.

1. Compute$\sigma_{\max}=\max_{k\geq r}(y(k)-y(k-r))$.

2. For each σ on the grid: build w_σ by (6), assemble $\Phi(\sigma)$, evaluate $\hat{\theta}(\sigma)$ by (1) and $J(\sigma)$ by (8).

3. Return $\hat{s}$ from (9) and $\hat{\theta}=\hat{\theta}(\hat{s})$.

The dominant cost is the construction of w_σ, giving $O(\sigma_{\max}\rho^{-1}N^2r^{-1})$ operations.

4.2 The estimate is an upper approximation

Proposition 1. *Let $\sigma=s$ and let the record be exact. Then $\hat{\theta}_l\geq\theta_l$ for every l, hence $\hat{h}\succeq h$, and for every input u' the model output satisfies $\hat{y}\succeq y$.*

Proof. By (7), $y(k)=\bigoplus_l\theta_l\otimes\Phi_l(k)\geq\theta_l\otimes\Phi_l(k)$ for every l and every k. In $\mathbb{Z}_{\max}$ this reads $y(k)-\Phi_l(k)\geq\theta_l$ whenever $\Phi_l(k)\neq\varepsilon$. Taking the minimum over k and using (1) gives $\hat{\theta}_l\geq\theta_l$. Since $\hat{p}_i\geq p_i$ and $\hat{q}_j\geq q_j$, isotony of $\oplus$ and $\otimes$ in (3) yields $\hat{h}\succeq h$, and isotony of (2) transfers the inequality to the outputs.

Proposition 1 states that the residuated estimator can never be optimistic. This is the algebraic reason why the criterion in (8) is a one-sided fit rather than a symmetric least-squares criterion, and it is the foundation of the robustness results of Section 4.6.

International Research Journal of Innovations in Engineering and Technology (IRJIET)

ISSN (online): 2581-3048

Volume 10, Issue 9, pp 150-163, September-2026

https://doi.org/10.47001/IRJIET/2026.109016

4.3 Exact recovery is equivalent to activation

Definition 1. The regressor Φ_l is *active* on the record if there exists $k\in\{0,\ldots,N-1\}$ with $\Phi_l(k)\neq\varepsilon$ and $\theta_l\otimes\Phi_l(k)=y(k)$; that is, if the l-th term attains the maximum in (7) at least once.

Theorem 2. *Let $\sigma=s$ and let the record be exact. Then $\hat{\theta}_l=\theta_l$ if and only if Φ_l is active.*

Proof. If Φ_l is active at index k then $y(k)-\Phi_l(k)=\theta_l$, so the minimum in (1) is at most θ_l; combined with Proposition 1 it equals θ_l. Conversely, if $\hat{\theta}_l=\theta_l$ then the minimum in (1) is attained at some index k, which gives $y(k)-\Phi_l(k)=\theta_l$, that is, activation.

Theorem 2 replaces the implicit richness condition of [15] by a criterion that is decidable in $O(N(v+r))$ operations once a candidate model is available. It also explains a phenomenon that is otherwise puzzling: the criterion J can vanish, meaning that the identified model reproduces the training record exactly, while individual parameters are wrong. A vanishing criterion certifies the fit, never the parameters.

4.4 Closed-form thresholds for constant-rate excitation

Consider the constant-rate input $u(k)=\delta k$, $\delta\geq0$, which corresponds to releasing parts at a fixed rate δ^{-1}.

Corollary 1 (transient block). *Under A1, for $1\leq i\leq v-1$ the coefficient p_i is recovered exactly if and only if*

$$\delta \leq \delta_i^{\max} := \min_{0\leq i' < i} \frac{p_i - p_{i'}}{i - i'},$$

and p_0 is always recovered exactly. Consequently the whole transient block is recovered if and only if $\delta\leq\delta^*:=\min_{1\leq i\leq v-1}\delta_i^{max}=p_1-p_0$.

Proof. Write $g(j)=p_j-\delta j$, so that the j-th transient term at index k equals $\delta k+g(j)$. At $k=0$ only Φ_0 is defined, hence p_0 is always active. For $0<i<v$ and $i\leq k$, activation of Φ_i at k requires $g(i)\geq g(j)$ for all $j\leq\min(k,v-1)$, and, once $k\geq v$, domination of the periodic block as well. Under A1 the map g is convex, so its maximum over the index window $\{0,\ldots,\min(k,v-1)\}$ is attained at an endpoint of that window. Therefore an interior index i can be active only when it is itself an endpoint, that is, at $k=i$. At $k=i$ the periodic block is absent (because $i<v$) and the competing terms are those with $j<i$, so activation holds if and only if $p_i-\delta i\geq p_j-\delta j$ for all $j<i$, which is (10). For $i=v-1$ the same inequality is obtained at $k=v-1$ and, when $k\geq v$, reduces to the case $j=0$, that is, to $\delta\leq(p_{v-1}-p_0)/(v-1)=\delta_{v-1}^{\max}$. Finally, under A1 the chord slopes $(p_i-p_0)/i$ are non-decreasing in i, so the minimum in (10) is attained at $i'=0$ and $\min_i\delta_i^{\max}=p_1-p_0$. Theorem 2 converts activation into exact recovery.

Corollary 2 (periodic block, *r*=1). *Under A1 and for $r=1$, the coefficient q_0 and the period duration s are recovered exactly if and only if $\delta\leq\lambda$ and the record is long enough in the sense of Proposition 3. If $\delta>\lambda$ then $w_s(k)=u(k)$, the periodic regressor becomes indistinguishable from the transient ones, and the selection rule (9) returns $\hat{s}=\delta$.*

Proof. From (6) with $r=1$ and $u(k)=\delta k$ one gets $w_\sigma(k)=\delta k+\max_{0\leq m\leq k}m(\sigma-\delta)$. For $\sigma=s>\delta$ the maximum is attained at $m=k$, giving $w_s(k)=sk$, a ray of slope $s>\delta$ that eventually dominates every transient term; the crossing index is computed in Proposition 3. For $s<\delta$ the maximum is attained at $m=0$, giving $w_s(k)=u(k)$, so column v of Φ duplicates a shifted copy of the transient columns and carries no information about s; the criterion J then vanishes for every $\sigma\leq\delta$ and (9) selects the largest such value, namely $\hat{s}=\delta$.

The two corollaries separate two thresholds that have often been merged. The transient block is limited by $\delta^*=p_1-p_0$, a quantity attached to the fastest route of the graph, whereas the periodic block is limited by the eigenvalue λ. In general $\delta^*\neq\lambda$, and complete identification requires $\delta\leq\min(\delta^*,\lambda)$. For the plant of Section V, $\delta^*=1$ while $\lambda=7$, so the binding constraint is seven times more demanding than the eigenvalue rule would suggest.

4.5 Minimum record length

Proposition 3. *Under A1 and for $r=1$ with constant-rate excitation $\delta<\lambda$, let*

$$K^* = \left\lceil \frac{s\,v - q_0 + \max_{0\leq i\leq v-1}(p_i - \delta i)}{s-\delta} \right\rceil$$

be the first index at which the periodic regressor dominates every transient regressor. Then complete exact identification requires

International Research Journal of Innovations in Engineering and Technology (IRJIET)

ISSN (online): 2581-3048

Volume 10, Issue 9, pp 150-163, September-2026

https://doi.org/10.47001/IRJIET/2026.109016

$$N \geq N_{\min} = \max\left(v,\ K^{*}\right) + r + 1.$$

Proof. By the proof of Corollary 2, the periodic term at index k equals $q_0+s(k-v)$ and the largest transient term equals $\delta k+\max_i(p_i-\delta i)$. Domination holds when $k(s-\delta)\geq sv-q_0+\max_i(p_i-\delta i)$, which is (11). The term v in (12) accounts for the v transient regressors, each of which becomes available only at its own index, and the additive $r+1$ reflects that the period duration is determined by a difference of two activations separated by r events, so the periodic block must be active at K^* and at K^*+r.

Since $K^*=\Theta((\lambda-\delta)^{-1})$, the required record length diverges as the release rate approaches the throughput limit of the plant. Away from that limit, (12) collapses to $N_{\min}=v+r+1$, one observation per parameter plus one. This resolves the apparent conflict between the intuition that longer records help and the empirical observation that they do not: both are correct, in different regimes.

4.6 Robustness to timestamp errors

Let $\tilde{y}=y+d$ be a perturbed record, where $d(k)$ is the error on the k-th output timestamp, and let $\|d\|_\infty=\max_k|d(k)|$.

Theorem 3 (non-expansiveness). *For every perturbation d and every σ,*

$$\left\|\hat{\theta}(\tilde{y})-\hat{\theta}(y)\right\|_\infty \leq \|d\|_\infty.$$

Moreover, if $\sigma=s$ and every regressor is active on the clean record, then $\|\hat{\theta}(\tilde{y})-\theta\|_\infty\leq\|d\|_\infty$.

Proof. For each l, $\hat{\theta}_l(\tilde{y})=\min_k(y(k)+d(k)-\Phi_l(k))$. A pointwise minimum of functions that are each translated by at most $\|d\|_\infty$ is itself translated by at most $\|d\|_\infty$, which gives (13). The second claim follows from Theorem 2, which gives $\hat{\theta}(y)=\theta$ under the stated activation hypothesis.

Corollary 3 (localisation). *Let $k_l^*\in\operatorname{argmin}_k(y(k)-\Phi_l(k))$ be the binding observation for parameter l, and let $m_l=\min_{k\neq k_l^*}(y(k)-\Phi_l(k))-\hat{\theta}_l$ be its slack margin. Any perturbation supported outside $\{k_l^*\}$ with $\|d\|_\infty<m_l$ leaves $\hat{\theta}_l$ unchanged.*

Proof. By (1), $\hat{\theta}_l$ is the minimum over k of $y(k)-\Phi_l(k)$. If the perturbation leaves k_l^* untouched and every other term is moved by less than its slack m_l, the index attaining the minimum is unchanged and so is its value.

Corollary 3 explains why perturbing different segments of the output record has radically different consequences: a parameter reacts only to the single observation that binds its constraint, and to perturbations of others only after the slack has been consumed.

Theorem 4 (guaranteed conservativeness). *Assume $\sigma=s$ and $d(k)\geq 0$ for every k, that is, timestamps are never recorded earlier than the true event. Then*

$$\theta \preccurlyeq \hat{\theta}(\tilde{y}) \preccurlyeq \theta\otimes\|d\|_\infty, \quad h \preccurlyeq \hat{h} \preccurlyeq h\otimes\|d\|_\infty.$$

In particular $\hat{h}\succeq h$: for every future input, the completion dates predicted by the identified model are never earlier than the true ones, and the pessimism is bounded by the worst-case timestamp error.

Proof. Isotony of $\tilde{y}\mapsto\Phi\backslash\tilde{y}$ and $d\geq 0$ give $\hat{\theta}(\tilde{y})\geq\hat{\theta}(y)$, and Proposition 1 gives $\hat{\theta}(y)\geq\theta$; this is the left inequality. The right inequality is Theorem 3 combined with the left one. The transfer inequalities follow by isotony of (3), and the statement about completion dates by isotony of (2).

Theorem 4 is what makes the estimator usable in practice. Timestamp acquisition in manufacturing execution systems is latency-bound: an event is registered when a sensor reading is processed, hence never before it occurs. Under that physically natural error model, the identified model is admissible for scheduling in the strong sense that any schedule proved feasible on the model is feasible on the plant, with a guaranteed pessimism margin. The assumption matters: Section V shows that symmetric errors destroy the property completely.

International Research Journal of Innovations in Engineering and Technology (IRJIET)

ISSN (online): 2581-3048

Volume 10, Issue 9, pp 150-163, September-2026

https://doi.org/10.47001/IRJIET/2026.109016

V. RESULTS AND DISCUSSION

5.1 Benchmark plants

The primary plant Σ_1, shown in Figure 1, is a kitting station fed by four parallel supply routes. Route i has lead time a_i and cycle time τ_i, with a=(10,8,4,4) and τ=(1,3,5,7); the fourth route carries one initial token. The output transition synchronises the four routes, so the transfer series is given by (15),

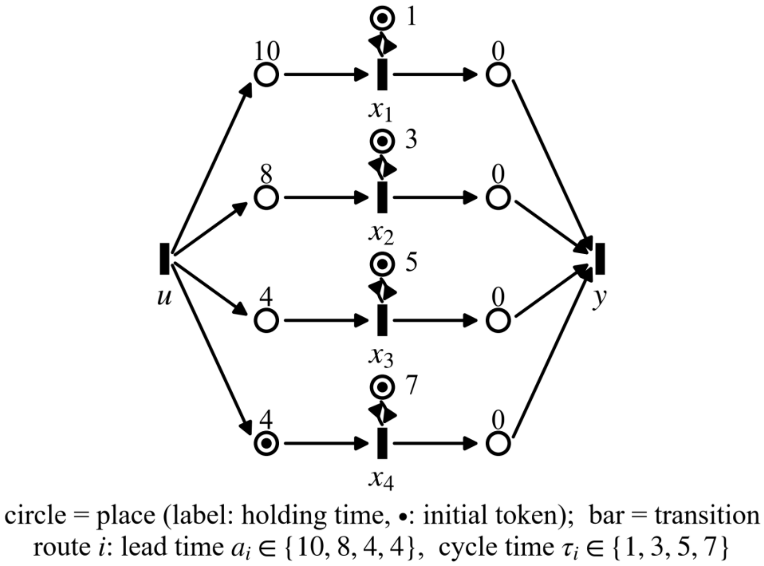

Figure 1: Benchmark plant Σ_1: a kitting station fed by four parallel supply routes. Circles are places, labelled with their holding time, and a dot indicates an initial token; bars are transitions. Route i has lead time a_i∈{10,8,4,4} and cycle time τ_i∈{1,3,5,7}. The output transition synchronises the four routes

$$h = 10(\gamma)^* \oplus 8(3\gamma)^* \oplus 4(5\gamma)^* \oplus 4\gamma(7\gamma)^*,$$

whose coefficients are h=(10,11,14,19,25,32,39,…). The canonical form (3) of the same plant is given by (16),

$$p = (10, 11, 14, 19), \quad q = (25), \quad s = 7, \quad r = 1, \quad v = 4, \quad \lambda = 7,$$

So that δ^*=p_1-p_0=1 and $\delta_i^{\max}$=(1,2,3) for i=1,2,3. Figure 2 shows the impulse response and its decomposition. The three parameterisations, direct TEG simulation, canonical form and simple-element sum, were verified to produce identical coefficient sequences. The same benchmark and its decomposition are used in a companion manuscript by the author [22], submitted to this journal in parallel.

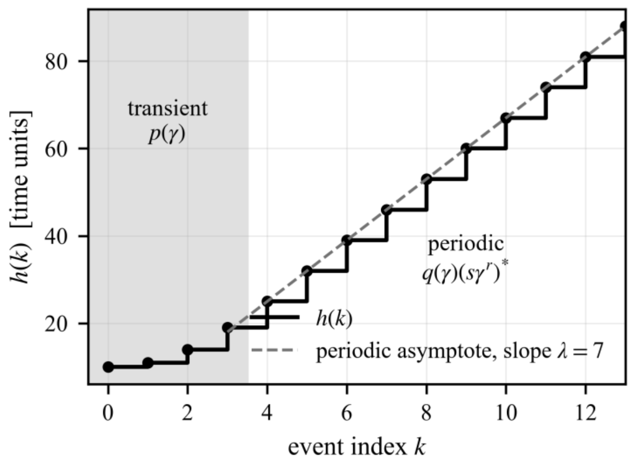

Figure 2: Impulse response of Σ_1 and its canonical decomposition. The shaded region is the transient block described by $p(\gamma)$; the dashed ray is the periodic asymptote of slope λ=7. The same figure appears in the companion manuscript [22]

International Research Journal of Innovations in Engineering and Technology (IRJIET)

ISSN (online): 2581-3048

Volume 10, Issue 9, pp 150-163, September-2026

https://doi.org/10.47001/IRJIET/2026.109016

A second plant Σ_2 with r=2 is used to check that the results are not an artefact of a unit period: p=(6,9,15), q=(20,26), s=12, r=2, hence λ=6 and δ^*=3.

Validation against a published example. Before the campaign, the implementation was checked against the worked example of [15]: with v=2, r=1, u=(0,5,9,15,19,21) and y=(17,22,26,32,37,43), Algorithm 1 returns $\hat{p}$=(17,21), $\hat{q}$=(25), $\hat{s}$=6 and J=0, reproducing the published values exactly.

5.2 Identifiability versus excitation rate

Constant-rate inputs $u(k)=\delta k$ with δ ranging over {0.25,0.50,…,15.00} were applied to Σ_1 with N=30. Table 1 lists representative outcomes and Figure 3 shows the complete map.

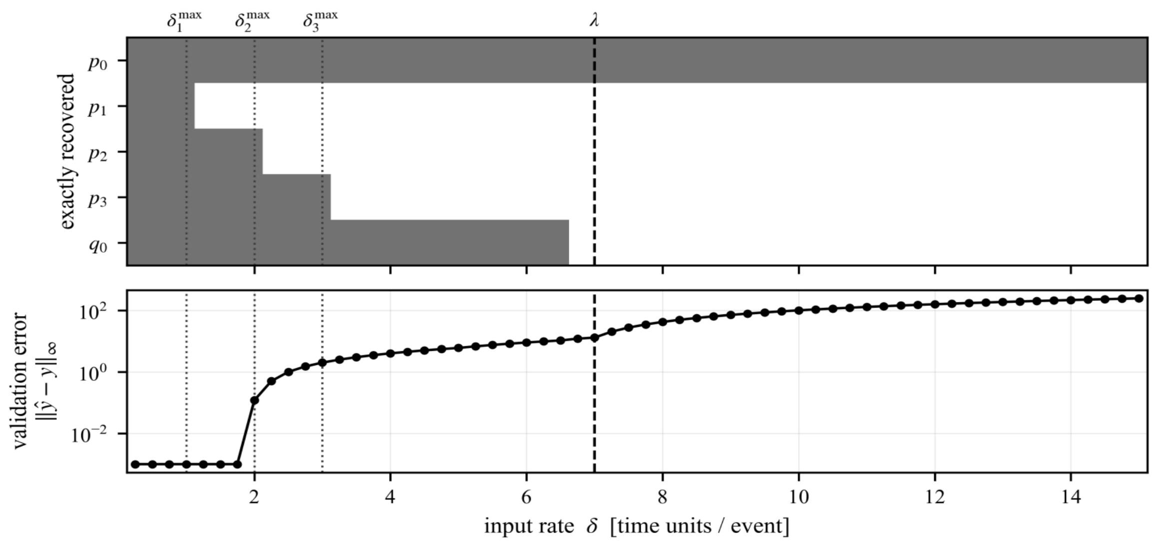

Figure 3: Identifiability map for constant-rate excitation. Top: shaded cells mark parameters recovered exactly; the dotted lines are the closed-form thresholds δ_i^{max}=(1,2,3) of Corollary 1 and the dashed line is the eigenvalue λ=7 of Corollary 2. Bottom: supremum-norm validation error on an independent input

Table 1: Exact recovery versus constant excitation rate, plant *Σ1, N=30*

δ	$\hat{p}_0$	$\hat{p}_1$	$\hat{p}_2$	$\hat{p}_3$	$\hat{q}_0$	$\hat{s}$	exact	val. err.
0.50	10.00	11.00	14.00	19.00	25.00	7.00	5/5	0.00
1.00	10.00	11.00	14.00	19.00	25.00	7.00	5/5	0.00
1.50	10.00	11.50	14.00	19.00	25.00	7.00	4/5	0.00
2.00	10.00	12.00	14.00	19.00	25.00	7.00	4/5	0.12
2.50	10.00	12.50	15.00	19.00	25.00	7.00	3/5	1.00
3.00	10.00	13.00	16.00	19.00	25.00	7.00	3/5	2.00
3.50	10.00	13.50	17.00	20.50	25.00	7.00	2/5	3.00
5.00	10.00	15.00	20.00	25.00	25.00	7.00	2/5	6.00
6.50	10.00	16.50	23.00	29.50	25.00	7.00	2/5	10.50
7.00	10.00	17.00	24.00	31.00	38.00	7.00	1/5	13.00
8.00	10.00	18.00	26.00	34.00	42.00	8.00	1/5	42.00
10.00	10.00	20.00	30.00	40.00	50.00	10.00	1/5	100.00
12.00	10.00	22.00	34.00	46.00	58.00	12.00	1/5	158.00

True values: θ=(10,11,14,19,25), s=7. Validation error is the supremum-norm output deviation on an independent random input of length 30.

Three observations follow. Coefficients drop out of identifiability one by one as δ increases, at exactly the rates δ_1^{max}=1, δ_2^{max}=2 and δ_3^{max}=3 predicted by Corollary 1. The periodic coefficient survives up to $\delta=\lambda$=7, at which point $\hat{q}_0$ jumps from 25 to 38 and, beyond it, $\hat{s}$ tracks δ exactly as predicted by Corollary 2. Finally, the training criterion J is zero for every rate in the table, including those where four of five parameters are wrong, which is the concrete manifestation of the warning after Theorem 2.

International Research Journal of Innovations in Engineering and Technology (IRJIET)

ISSN (online): 2581-3048

Volume 10, Issue 9, pp 150-163, September-2026

https://doi.org/10.47001/IRJIET/2026.109016

Table 2 summarises how well the two criteria of Section III account for the whole sweep and for the second plant.

Table 2: Agreement of the identifiability criteria

criterion	plant	agreement
activation (Theorem 2)	Σ_1, 60 rates	60 / 60
closed form (Corollaries 1 and 2)	Σ_1, 60 rates	59 / 60
closed form (Corollaries 1 and 2)	Σ_2, 9 rates	9 / 9

The activation criterion reproduces the observed pattern of exact recovery without a single discrepancy. The one closed-form mismatch occurs at δ=6.75, where the record length N=30 falls below the requirement (12), which is $N_{\min}$=54; this is a horizon effect rather than an identifiability effect and is examined next.

Table 3 compares canonical excitation strategies. The impulse, which is the classical choice, is optimal but is also the least realisable in practice, since it requires an unbounded burst of releases at time zero. Any constant release rate below δ^* achieves the same result and is directly implementable.

Table 3: Excitation strategies, plant Σ_1, N=30

excitation	exact	$\hat{s}$	J	val. err.
impulse, u=e	5/5	7.00	0.00	0.00
constant rate δ=0.5	5/5	7.00	0.00	0.00
constant rate δ=1.0=δ^*	5/5	7.00	0.00	0.00
constant rate δ=2.0	4/5	7.00	0.00	0.00
constant rate δ=5.0	2/5	7.00	0.00	6.00
constant rate δ=7.0=λ	1/5	7.00	0.00	13.00
constant rate δ=10.0>λ	1/5	10.00	0.00	130.00
random, mean 3, spread 2.5	2/5	7.00	0.00	1.23
random, mean 8, spread 7.5	4/5	7.00	0.00	0.00

The last two rows deserve comment. A random release schedule with mean gap 8, which exceeds the eigenvalue, nevertheless recovers four parameters, because its individual gaps fluctuate down into the identifiable band. Mean rate alone is therefore not the right descriptor; what matters is whether the gap sequence visits the intervals prescribed by Corollary 1.

5.3 Minimum record length

For each rate, the smallest N giving exact recovery of the periodic block was determined by exhaustive search. Table 4 compares it with (12) and Figure 4 plots both against λ-δ.

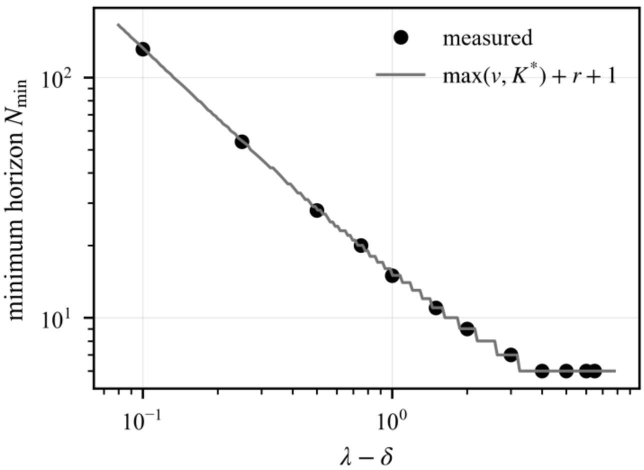

Figure 4: Minimum record length versus the distance from the eigenvalue. Markers are exhaustive-search measurements; the line is the closed-form law (12)

International Research Journal of Innovations in Engineering and Technology (IRJIET)

ISSN (online): 2581-3048

Volume 10, Issue 9, pp 150-163, September-2026

https://doi.org/10.47001/IRJIET/2026.109016

Table 4: Minimum record length, plant Σ_1

δ	λ-δ	K^*	N_{min} predicted	N_{min} measured
0.50	6.50	4	6	6
1.00	6.00	4	6	6
2.00	5.00	4	6	6
3.00	4.00	4	6	6
4.00	3.00	5	7	7
5.00	2.00	7	9	9
5.50	1.50	9	11	11
6.00	1.00	13	15	15
6.25	0.75	18	20	20
6.50	0.50	26	28	28
6.75	0.25	52	54	54
6.90	0.10	130	132	131

The law is exact in eleven of twelve cases on Σ_1 and in seven of seven on Σ_2, eighteen of nineteen overall. The single exception, δ=6.90, is a degenerate configuration in which the transient and periodic envelopes intersect exactly at an integer index, so that activation occurs by equality rather than strict domination and one observation is saved.

The practical reading of Table 4 is that a record of six observations suffices to identify a five-parameter model when the plant is driven at less than half its throughput limit, whereas one hundred and thirty-one observations are needed at ninety-nine per cent of the limit. Reports that record length is immaterial are correct only in the first regime.

5.4 Propagation of timestamp errors

With $\hat{s}$ fixed at its true value to isolate the effect on θ, a constant offset ε was added to the output record over three supports: the transient block $k<v+r$, the periodic block $k\geq v+r$, and the whole record. Table 5 reports the resulting parameter shifts and Figure 5 plots them.

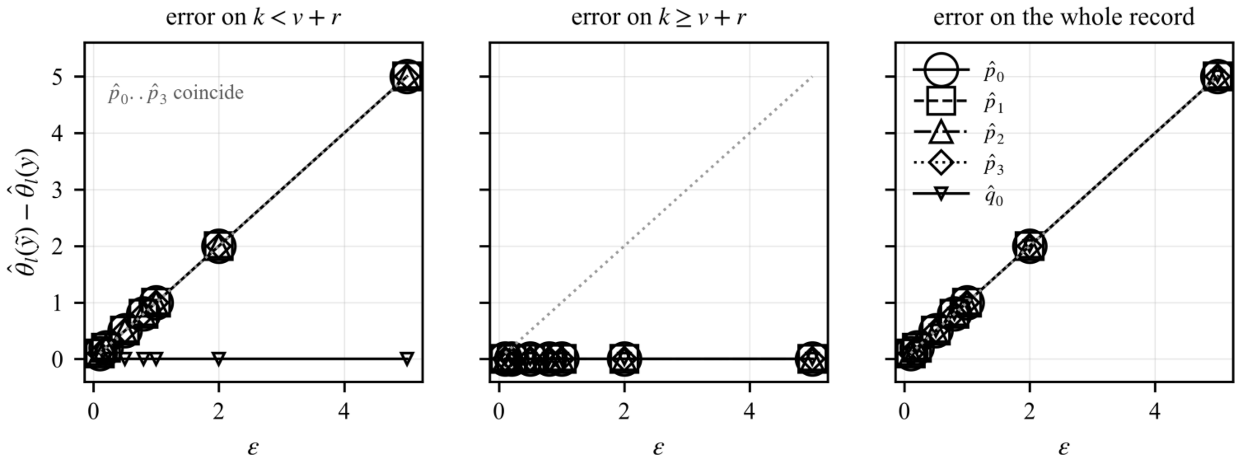

Figure 5: Propagation of a constant timestamp offset ε applied to the transient block, the periodic block and the whole record. The four transient estimates coincide. The grey diagonal is the bound of Theorem 3, which is attained

Table 5: Timestamp-error propagation, plant Σ_1, $u(k)=k$

ε	support	$\Delta\hat{p}_0$	$\Delta\hat{p}_1$	$\Delta\hat{p}_2$	$\Delta\hat{p}_3$	$\Delta\hat{q}_0$	ratio
0.2	transient	0.20	0.20	0.20	0.20	0.00	1.00
0.2	periodic	0.00	0.00	0.00	0.00	0.00	0.00
0.2	whole	0.20	0.20	0.20	0.20	0.20	1.00

International Research Journal of Innovations in Engineering and Technology (IRJIET)

ISSN (online): 2581-3048

Volume 10, Issue 9, pp 150-163, September-2026

https://doi.org/10.47001/IRJIET/2026.109016

0.8	transient	0.80	0.80	0.80	0.80	0.00	1.00
0.8	periodic	0.00	0.00	0.00	0.00	0.00	0.00
0.8	whole	0.80	0.80	0.80	0.80	0.80	1.00
2.0	transient	2.00	2.00	2.00	2.00	0.00	1.00
2.0	periodic	0.00	0.00	0.00	0.00	0.00	0.00
2.0	whole	2.00	2.00	2.00	2.00	2.00	1.00
5.0	transient	5.00	5.00	5.00	5.00	0.00	1.00
5.0	periodic	0.00	0.00	0.00	0.00	0.00	0.00
5.0	whole	5.00	5.00	5.00	5.00	5.00	1.00

Ratio is $\|\Delta\theta\|_\infty/\varepsilon$; the theoretical bound of Theorem 3 is 1.

The binding observations for the five parameters are k^*=(0,1,2,3,4), all inside the transient block. Corollary 3 therefore predicts exactly what is measured: an error confined to the periodic block leaves every parameter untouched, an error on the transient block shifts every parameter by the full amount except $\hat{q}_0$, whose binding index is k=4, and an error on the whole record shifts all five. The bound of Theorem 3 is attained, so it cannot be improved. Over three thousand random jitter realisations the largest observed ratio was also exactly 1.000.

This refines the qualitative observation, reported in earlier empirical work, that errors on the later part of the record do not appear in the transient parameters. The mechanism is not a property of the transient and periodic blocks as such but of the location of the binding observations, which the estimator makes explicit and which can therefore be computed in advance.

5.5 Stratified Monte-Carlo study

Two thousand four hundred runs were performed with record length drawn from {8,12,16,20,28}, random release schedules with mean gap uniform on [0.05,12], and symmetric jitter $d(k)$~$U(-\varepsilon,\varepsilon)$ with ε~$U(0,2)$. Runs were stratified by the realised mean rate. Table 6 reports the outcome and Figure 6 summarises it.

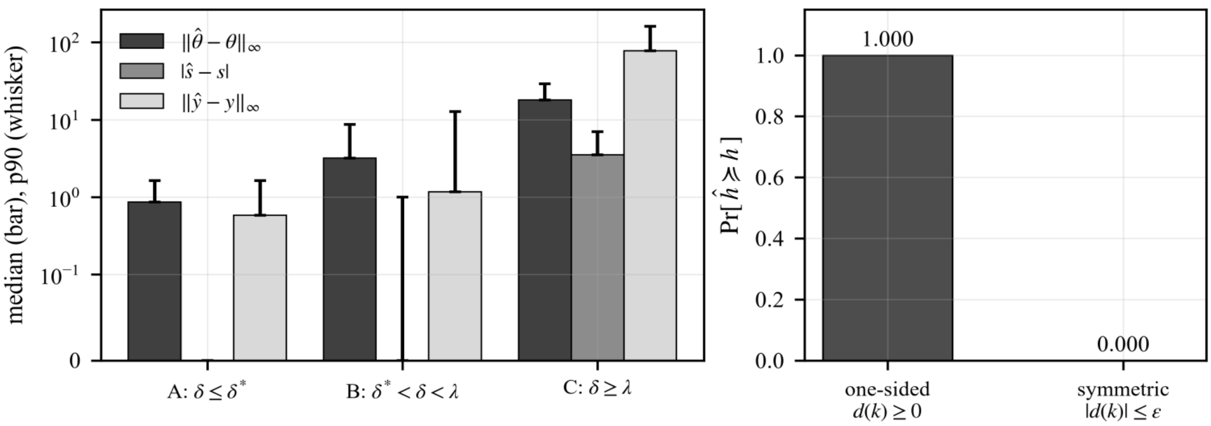

Figure 6: Left: stratified Monte-Carlo results, bars are medians and whiskers reach the ninetieth percentile. Right: probability that the identified model dominates the true one, under one-sided and symmetric timestamp errors

Table 6: Stratified Monte-Carlo, 2400 runs, plant Σ_1

stratum	runs	param. err. median	param. err. p95	period err. median	valid. err. median	valid. err. p95	Pr[ŝ = s]
A: $\delta \le \delta^*$	172	0.863	1.796	0.000	0.583	10.002	0.913
B: $\delta^* < \delta < \lambda$	1236	3.192	10.252	0.000	1.170	26.361	0.760
C: $\delta \ge \lambda$	992	17.973	42.899	3.500	77.916	182.466	0.026

The upper-approximation property of Proposition 1 held in 2400 of 2400 runs, and the empirical Lipschitz constant of Theorem 3 reached its theoretical value of 1.000. Parameter error in stratum A is of the order of the injected jitter, as (13) requires.

International Research Journal of Innovations in Engineering and Technology (IRJIET)

ISSN (online): 2581-3048

Volume 10, Issue 9, pp 150-163, September-2026

https://doi.org/10.47001/IRJIET/2026.109016

Degradation across strata is severe: the median validation error grows by two orders of magnitude between A and C, and the period duration is recovered in only 2.6 per cent of runs once the plant is driven at or beyond its throughput limit.

5.6 Error model and conservativeness

The dichotomy predicted by Theorem 4 was tested by repeating the Monte-Carlo study inside the identifiable band with two error models: one-sided, $d(k)\sim U(0,\varepsilon)$, and symmetric, $d(k)\sim U(-\varepsilon,\varepsilon)$.

Table 7: Error model and guaranteed conservativeness, 2400 runs each

error model	Pr[ŝ = s]	Pr[model dominates]	Pr[bound (13) holds]	mean param. err.	mean pessimism	max pessimism
one-sided, $d(k)\geq 0$	1.000	**1.000**	1.000	0.784	0.712	1.966
symmetric, $-\varepsilon\leq d(k)\leq\varepsilon$	0.987	**0.000**	1.000	0.945	0.512	10.597

The separation is complete. Under latency-bound timestamps the identified model dominated the true model in every single run, with mean pessimism 0.712 time units and worst case 1.966, both consistent with the sandwich bound (14) for $\|d\|_\infty\leq 2$. Under symmetric errors the property failed in every run, and although the average deviation is smaller the worst-case optimism reaches 10.6 time units, which for a scheduling application means an infeasible plan.

The bound of Theorem 3 was respected in 100 per cent of runs under both models. Figure 7 shows representative trajectories inside and outside the identifiable band.

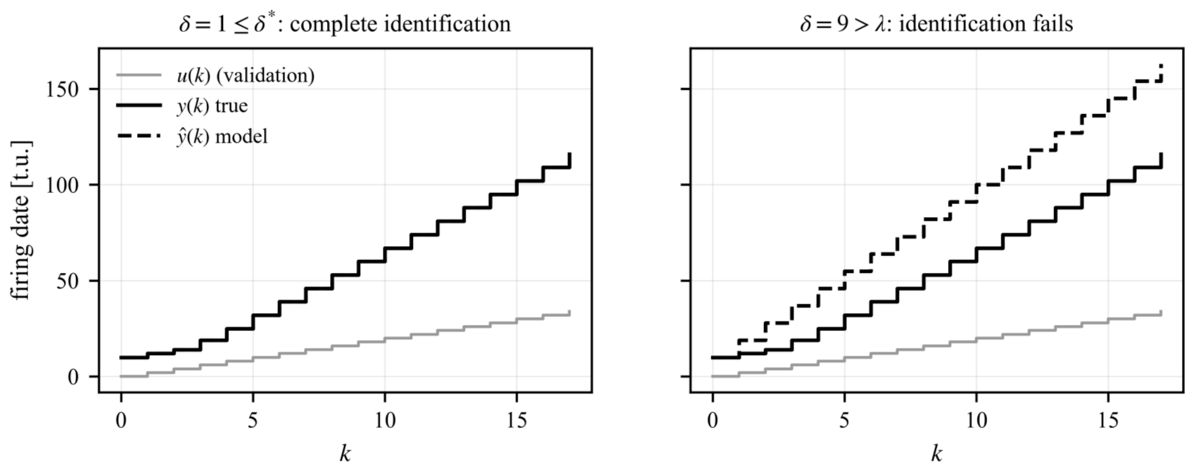

Figure 7: Representative validation trajectories inside the identifiable band (δ=1) and outside it (δ=9), evaluated on a common independent input

5.7 Design guidelines

The results translate into four concrete rules for an identification experiment on a max-plus linear plant.

Rule 1: release below the fastest transient slope, not below the eigenvalue. Complete identification requires $\delta\leq\min(\delta^*,\lambda)$ with $\delta^*=p_1-p_0$. Since δ^* is attached to the fastest route while λ is attached to the bottleneck, the two can differ by a large factor; on Σ_1 the ratio is seven. Designing the experiment on the eigenvalue alone leaves the transient block unidentifiable while producing a criterion equal to zero, which is a silent failure.

Rule 2: prefer a slow constant rate to an impulse. Table 3 shows that any constant rate at or below δ^* matches the impulse exactly. Since an impulse requires an unbounded release burst and a slow constant rate does not, there is no reason to insist on the impulse response, which removes the main practical objection to residuation-based identification.

Rule 3: size the record from (12), not from a rule of thumb. Six observations suffice at half the throughput limit; one hundred and thirty-one are needed at ninety-nine per cent of it. Since $N_{\min}$ can be evaluated from a preliminary coarse model, the experiment can be sized before it is run.

ISSN (online): 2581-3048
Volume 10, Issue 9, pp 150-163, September-2026
https://doi.org/10.47001/IRJIET/2026.109016

Rule 4: keep timestamps latency-bound. If the acquisition chain can be guaranteed never to report an event before it occurs, Theorem 4 provides a hard guarantee that the identified model is admissible for scheduling. If timestamps are corrected symmetrically, for instance by a clock-synchronisation filter that can advance a reading, the guarantee is lost; Table 7 shows the failure is not marginal but total. Where symmetric noise cannot be avoided, conservativeness can be restored by inflating the identified parameters by the known error bound, at the cost of the pessimism quantified in (14). An alternative is to carry the bound explicitly and work with an interval model, for which reachability and control results already exist [11], [21].

VI. CONCLUSION

Residuation-based identification of max-plus linear discrete event systems always returns a model, and the criterion it minimises can vanish while most parameters are wrong. That criterion is replaced here by a decidable exactness test: a parameter is recovered if and only if its regressor attains the maximum in the measured output at least once. For constant-rate excitation the test yields closed-form critical rates, showing that the transient block is limited by the fastest chord slope of the transient sequence and the periodic block by the eigenvalue, two thresholds that are generally different. The minimum record length was obtained in closed form and diverges as the release rate approaches the throughput limit. The estimator was proved non-expansive with respect to timestamp errors, and under latency-bound timestamps the identified model dominates the true one, so predicted completion dates are never optimistic. More than seven thousand runs on two plants confirmed every statement.

VII. FUTURE SCOPE

The analysis assumes the structural indices v and r known, as does the estimator itself. Corollaries 1 and 2 assume a convex transient and, for the closed forms, a unit period and a constant-rate input; the activation criterion of Theorem 2, which is the primitive result, requires none of these. Extending the closed forms to $r>1$ and to general non-uniform excitation is the natural continuation, as is the joint estimation of the structural indices by embedding Algorithm 1 in a search over (v,r) scored by an out-of-sample criterion rather than by J, which Section 5.2 shows to be uninformative about parameter accuracy.

Two further directions follow from the results. The excitation design rules were derived for a single-input single-output graph; the residuated formulation itself extends to the matrix case, so the identifiability analysis could be repeated there. And where symmetric timestamp noise cannot be avoided, the sandwich bound (14) suggests carrying the error bound explicitly and identifying an interval model instead of a point estimate, for which reachability and control results already exist [11], [21].

ACKNOWLEDGEMENT

The work reported here grew out of a master's study on the identification of discrete event systems carried out at the Institut de Recherche en Communications et Cybernétique de Nantes under the supervision of Claude Martinez, whom the author thanks. Thanks are due also to Pierre Castagna, Muriel Gapaillard and Rosa Abbou for their comments on that earlier study.

REFERENCES

[1] F. Baccelli, G. Cohen, G. J. Olsder, and J.-P. Quadrat, Synchronization and Linearity: An Algebra for Discrete Event Systems. *Chichester, U.K.: Wiley,* 1992.
[2] B. Heidergott, G. J. Olsder, and J. van der Woude, Max Plus at Work: Modeling and Analysis of Synchronized Systems. *Princeton, NJ: Princeton Univ. Press,* 2006.
[3] R. A. Cuninghame-Green, Minimax Algebra, Lecture Notes in Economics and Mathematical Systems, vol. 166. *Berlin, Germany: Springer-Verlag,* 1979, doi: 10.1007/978-3-642-48708-8.
[4] B. Cottenceau, L. Hardouin, J.-L. Boimond, and J.-L. Ferrier, "Model reference control for timed event graphs in dioids," *Automatica,* vol. 37, no. 9, pp. 1451–1458, 2001, doi: 10.1016/S0005-1098(01)00073-5.
[5] B. De Schutter and T. van den Boom, "Model predictive control for max-plus-linear discrete event systems," *Automatica,* vol. 37, no. 7, pp. 1049–1056, 2001, doi: 10.1016/S0005-1098(01)00054-1.
[6] J. Xu, T. van den Boom, and B. De Schutter, "Model predictive control for stochastic max-plus linear systems with chance constraints," *IEEE Trans. Autom. Control,* vol. 64, no. 1, pp. 337–342, 2019, doi: 10.1109/TAC.2018.2849570.
[7] L. Hardouin, C. A. Maia, B. Cottenceau, and M. Lhommeau, "Observer design for (max, plus) linear systems," *IEEE Trans. Autom. Control,* vol. 55, no. 2, pp. 538–543, 2010, doi: 10.1109/TAC.2009.2037477.
[8] L. Hardouin, Y. Shang, C. A. Maia, and B. Cottenceau, "Observer-based controllers for max-plus linear systems," *IEEE Trans. Autom. Control,* vol. 62, no. 5, pp. 2153–2165, 2017, doi: 10.1109/TAC.2016.2604562.

ISSN (online): 2581-3048
Volume 10, Issue 9, pp 150-163, September-2026
https://doi.org/10.47001/IRJIET/2026.109016

[9] C. A. Maia, C. R. Andrade, and L. Hardouin, "On the control of max-plus linear system subject to state restriction," *Automatica*, vol. 47, no. 5, pp. 988–992, 2011, doi: 10.1016/j.automatica.2011.01.047.

[10] Y. Shang, L. Hardouin, M. Lhommeau, and C. A. Maia, "An integrated control strategy to solve the disturbance decoupling problem for max-plus linear systems with applications to a high throughput screening system," *Automatica*, vol. 63, pp. 338–348, 2016, doi: 10.1016/j.automatica.2015.10.030.

[11] M. Lhommeau, L. Hardouin, B. Cottenceau, and L. Jaulin, "Interval analysis and dioid: Application to robust controller design for timed event graphs," *Automatica*, vol. 40, no. 11, pp. 1923–1930, 2004, doi: 10.1016/j.automatica.2004.05.013.

[12] T. Brunsch, L. Hardouin, C. A. Maia, and J. Raisch, "Duality and interval analysis over idempotent semirings," *Linear Algebra Appl.*, vol. 437, no. 10, pp. 2436–2454, 2012, doi: 10.1016/j.laa.2012.06.025.

[13] F. Gallot, J.-L. Boimond, and L. Hardouin, "Identification of simple elements in max-algebra: Application to SISO discrete event systems modelisation," *in Proc. European Control Conf. (ECC), Brussels, Belgium*, 1997, pp. 1866–1871, doi: 10.23919/ECC.1997.7082376.

[14] L. Hardouin, E. Menguy, J.-L. Boimond, and J.-L. Ferrier, "SISO discrete event systems control in dioid algebra," *J. Européen des Systèmes Automatisés*, vol. 31, no. 3, pp. 433–452, 1997.

[15] C. A. Maia, R. Santos-Mendes, and L. Hardouin, "Some results on identification of timed event graphs in dioid," 2003.

[16] T. S. Blyth and M. F. Janowitz, Residuation Theory. *Oxford, U.K.: Pergamon Press,* 1972, doi: 10.1016/B978-0-08-016408-3.50004-8.

[17] G. Cohen, "Residuation and applications," in Algèbres Max-Plus et Applications en Informatique et Automatique, *École de Printemps d'Informatique Théorique, Noirmoutier, France: INRIA*, 1998.

[18] S. Klein, L. Litz, and J.-J. Lesage, "Fault detection of discrete event systems using an identification approach," *IFAC Proc. Volumes (16th IFAC World Congress)*, vol. 38, no. 1, pp. 92–97, 2005, doi: 10.3182/20050703-6-CZ-1902.01440.

[19] L. Ljung, System Identification: Theory for the User, *2nd ed. Upper Saddle River, NJ: Prentice-Hall*, 1999.

[20] S. Gaubert, "Théorie des systèmes linéaires dans les dioïdes," *Ph.D. dissertation, École des Mines de Paris, France*, 1992.

[21] R. M. F. Cândido, L. Hardouin, M. Lhommeau, and R. S. Santos Mendes, "Conditional reachability of uncertain max-plus linear systems," *Automatica*, vol. 94, pp. 426–435, 2018, doi: 10.1016/j.automatica.2017.11.030.

[22] G. Aryan, "A unified residuation framework for the identification of max-plus linear systems: moving-average, recursive and structural estimation," *manuscript submitted to the International Research Journal of Innovations in Engineering and Technology (IRJIET)*, 2026.

Citation of this Article:

Ghadir Aryan. (2026). Excitation Design and Guaranteed Robustness Bounds for Residuation-Based Identification of Max-Plus Linear Discrete Event Systems. *International Research Journal of Innovations in Engineering and Technology - IRJIET*, 10(9), 150-163. Article DOI https://doi.org/10.47001/IRJIET/2026.109016

****